PIO I-II tendencies. Part 2. Improving the pilot modeling

Adrian TOADER*, Ioan URSU*

*Corresponding author
INCAS - National Institute for Aerospace Research "Elie Carafoli"
220, Iuliu Maniu Bdlv, Bucharest 061126, Romania
iursu@incas.ro

DOI: 10.13111/2066-8201.2011.3.1.15

Abstract: *The study is conceived in two parts and aims to get some contributions to the problem of PIO aircraft susceptibility analysis. Part I, previously published in this journal, highlighted the main steps of deriving a complex model of human pilot. The current Part II of the paper considers a proper procedure of the human pilot mathematical model synthesis in order to analyze PIO II type susceptibility of a VTOL-type aircraft, related to the presence of position and rate-limited actuator. The mathematical tools are those of semi global stability theory developed in recent works.*

Key Words: LQG control, optimal model of human pilot, PIO, actuator position and rate saturation

1. INTRODUCTION

"**P**ilot-**I**nduced-**O**scillation" (PIO) is a phenomenon usually due to adverse aircraft-pilot coupling during some tasks in which "tight closed loop control of the aircraft is required from the pilot, with the aircraft not responding to the pilot commands as expected by the pilot himself" [1]. Predicting PIO is difficult and becomes even more difficult with the development of new technologies such as the active control and fly-by-wire flight control systems. According to common references (see, for example, [2]), PIOs are categorized depending essentially on the degree of nonlinearity in the event.

Undoubtedly, to have at hand a mathematical model of pilot behavior is very important for deriving a PIO prognostic theory. Part I of the present study [3] highlighted the main steps of designing a complex model – Modified Optimal Control Model (MOCM) – for the human pilot based on the work [4]. The numerical validation of this model was performed in the concrete case of a hovering VTOL-type aircraft analyzed in the classical reports [5]-[8] from the viewpoint of the *robust stability analysis criterion for PIO I prediction* [9].

A recent paper of the authors [10] has investigated the susceptibility of the tandem pilot-aircraft system to PIO generated by the actuator rate saturation. The classical Popov and circle criteria [11] didn't work as applied to this model, given the conservativeness of the criteria, which provide only the sufficient stability conditions. The question has been surpassed by appealing to a weaker circle criterion [12].

The present Part II of our study on PIO phenomenon enlarges the interest to the consideration of whole realistic case of both position and rate-limited actuator saturations. The mathematical tools will be those of semi global stability theory developed and applied in recent works [13]-[16]. Unfortunately, the MOCM mathematical model is not suitable given the constraints of the semi global stabilization theory. To face it out, we applied once again the conjecture of the mathematical models flexibility [17]: instead of MOCM of human pilot [3], the Hess-LQG (HLQG) based pilot model (see also [4]), will be used. This is compatible with the mechanism of the semi global stabilization theory. This topic of research started from the seminal paper [14], where it was established that a linear system subject to actuator position saturation can be globally asymptotically stabilized – by nonlinear feedback – if and only if the system in the absence of the saturation is asymptotically null controllable with bounded controls. The notion "asymptotically null controllable with bounded controls" is equivalent [18] to the usual notion of linear stabilizability plus the added condition that all the open-loop poles be in the closed-left plane. A related result is that, in general, linear feedback cannot achieve global asymptotic stabilization [19]. Thus, given this negative result, the notion of "semi global stabilization theory for systems subject to input saturation" is introduced in [14].

The remainder of the paper is organized as follows. Firstly, in Section 2, a proper model of the human pilot is presented, nearly following [4]. Then, in Section 3, the semi global stabilization theory is suited in order to study the prevention of aircraft PIO II tendencies in the presence of the realistic position and rate actuator saturations. In Section 4, some numerical simulations are presented. A conclusive Section 5 underlines the interest of our approach in the prominence of PIOs.

2. DESCRIPTION OF THE HESS'S LQG PILOT MODEL SYNTHESIS

The aircraft dynamics is written in the form of well known invariant linear system, see [3]

$$\dot{x} = Ax + B\delta + Ew,\ y_o = Cx + D\delta + v_y := y + v_y \tag{1}$$

There are some usual pilot models: the HLQG model, LQG model, optimal control model (OCM) and the modified optimal control model [4]. From technical – methodological – reasons, the HLQG model will be herein considered. This was initially a structural model [20], composed of two blocks: the central nervous block and the neuromuscular block (Fig. 1). Both are of delay type: first is modeled by the transfer function

$$\frac{u_p}{u_c} = \frac{\left(s - 4/\tau\right)^2}{\left(s + 4/\tau\right)^2} \tag{2}$$

(τ is the delay, u_p is the pilot's delayed control input, u_c is the pilot's commanded control) and the second is modeled by the lag block

$$\frac{\delta}{u_d} = \frac{1}{\tau_\eta s + 1},\ u_d = u_p + v_u \tag{3}$$

Both the blocks are placed in Fig. 1 at the pilot's output and methodologically will be considered as part of the plant dynamics. The two blocks, in state space form, are given by

$$\begin{bmatrix} \dot{x}_{d_1} \\ \dot{x}_{d_2} \\ \dot{\delta} \end{bmatrix} = \begin{bmatrix} 0 & -16/\tau^2 & 0 \\ 1 & -8/\tau & 0 \\ 0 & 1/\tau_\eta & -1/\tau_\eta \end{bmatrix} \begin{bmatrix} x_{d_1} \\ x_{d_2} \\ \delta \end{bmatrix} + \begin{bmatrix} 0 \\ -16/\tau \\ 1/\tau_\eta \end{bmatrix} u_c + \begin{bmatrix} 0 \\ 0 \\ 1/\tau_\eta \end{bmatrix} v_u,\ \delta = \begin{bmatrix} 0 & 0 & 1 \end{bmatrix} \begin{bmatrix} x_{d_1} \\ x_{d_2} \\ \delta \end{bmatrix} \tag{4}$$

or, in matrix form

$$\dot{x}_d = A_d x_d + B_d u_c + E_d v_u,\ \delta = C_d x_d \tag{4′}$$

The dynamics (1), (4′) are then concatenated as extended plant dynamics

$$\begin{bmatrix} \dot{x} \\ \dot{x}_d \end{bmatrix} = \begin{bmatrix} A & BC_d \\ 0 & A_d \end{bmatrix} \begin{bmatrix} x \\ x_d \end{bmatrix} + \begin{bmatrix} 0 \\ B_d \end{bmatrix} u_c + \begin{bmatrix} E & 0 \\ 0 & E_d \end{bmatrix} \begin{bmatrix} w \\ v_u \end{bmatrix}, y = \begin{bmatrix} C & DC_d \end{bmatrix} \begin{bmatrix} x \\ x_d \end{bmatrix} \tag{5}$$

or, in matrix form

$$\dot{x}_s = A_s x_s + B_s u_c + E_s w_1, y = C_s x_s, y_0 = C_s x_s + v_y \tag{5$'$}$$

The approach of pilot modeling is based on the argument, experimentally proved, that the pilot behaves “optimally”, more exactly, in the terms of the LQG paradigm, aims to minimize the index

$$J_p = \mathrm{E}_\infty \left\{ y^{\mathrm{T}} Q_y y + (u_c)^{\mathrm{T}} r u_c \right\} \tag{6}$$

subject to pilot observations y_o, with cost function weights $Q_y \geq 0$ [4] and $r > 0$.

The minimizing of the control law is obtained by the application of LQG solution techniques to the augmented system. This leads to the full-state feedback relation

$$u_c = -g_p \hat{x}_s = -r^{-1} B_s^{\mathrm{T}} K \hat{x}_s \tag{7}$$

where $\hat{x}_s$ is the estimate of the state x_s and K is the unique positive definite solution of the matrix Ricatti equation

$$0 = A_s^{\mathrm{T}} K + K A_s + Q - K B_s r^{-1} B_s^{\mathrm{T}} K \tag{8}$$

where $Q = C_s^{\mathrm{T}} Q_y C_s$.

The current estimate of the state is given by a Kalman filter

$$\dot{\hat{x}}_s = A_s \hat{x}_s + B_s u_c + F(y_o - \hat{y}), \dot{\hat{x}}_s = (A_s - FC_s)\hat{x}_s + FC_s x_s + B_s u_c + F v_y, F = S C_s^{\mathrm{T}} V_y^{-1} \tag{9}$$

The covariance matrix of the estimation error S is the unique positive definite solution of the matrix Ricatti equation

$$0 = \boldsymbol{A}_s S + S A_s^T + W_1 - S C_s^{\mathrm{T}} V_y^{-1} \boldsymbol{C}_s S \tag{10}$$

where the covariance matrix W_1 is a diagonal of covariance matrices $W_1 = \mathrm{diag}(W, V_u)$.

Consequently, the state space representation of the closed-loop system is given by

$$\begin{bmatrix} \dot{x}_s \\ \dot{\hat{x}}_s \end{bmatrix} = \begin{bmatrix} A_s & -B_s g_p \\ FC_s & A_s - B_s g_p - FC_s \end{bmatrix} \begin{bmatrix} x_s \\ \hat{x}_s \end{bmatrix} + \begin{bmatrix} E_s & 0 \\ 0 & F \end{bmatrix} \begin{bmatrix} w_1 \\ v_y \end{bmatrix}, \begin{bmatrix} \boldsymbol{y}_0 \\ u_c \end{bmatrix} = \begin{bmatrix} \boldsymbol{C}_s & 0 \\ 0 & -g_p \end{bmatrix} \begin{bmatrix} x_s \\ \hat{x}_s \end{bmatrix} + \begin{bmatrix} v_y \\ 0 \end{bmatrix} \tag{11}$$

$$\dot{x}_{cl} = A_{cl} x_{cl} + E_{cl} w, Y = C_{cl} x_{cl} + \tilde{v}_y$$

$$A_{cl} := \begin{bmatrix} A_s & -B_s g_p \\ FC_s & A_s - B_s g_p - FC_s \end{bmatrix}, E_{cl} := \begin{bmatrix} E_s & 0 \\ 0 & F \end{bmatrix}, C_{cl} := \begin{bmatrix} C_s & 0 \\ 0 & -g_p \end{bmatrix} \tag{11$'$}$$

The pilot’s dynamics is represented by

$$\begin{bmatrix} \dot{\hat{x}}_s \\ \dot{x}_d \end{bmatrix} = \begin{bmatrix} A_s - B_s g_p - FC_s & 0 \\ -B_d g_p & A_d \end{bmatrix} \begin{bmatrix} \hat{x}_s \\ x_d \end{bmatrix} + \begin{bmatrix} F \\ 0 \end{bmatrix} y + \begin{bmatrix} F & 0 \\ 0 & E_d \end{bmatrix} \begin{bmatrix} v_y \\ v_u \end{bmatrix}, \delta = \begin{bmatrix} 0 & \boldsymbol{C}_d \end{bmatrix} \begin{bmatrix} \hat{x}_s \\ x_d \end{bmatrix} \quad (12)$$

or, in matrix form

$$\dot{x}_p = A_p x_p + B_p y + E_p v_p, \delta = C_p x_p \quad (12')$$

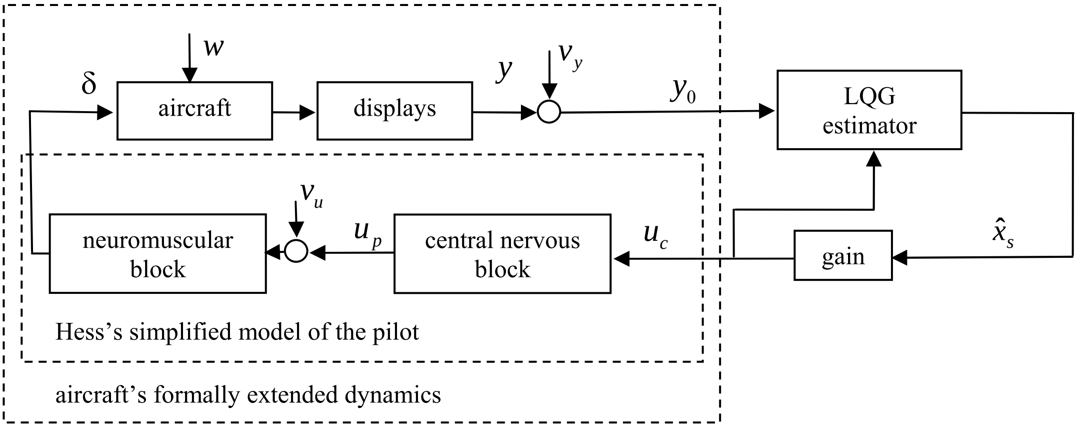

Fig. 1 – Conceptual block diagram of the human pilot dynamic model

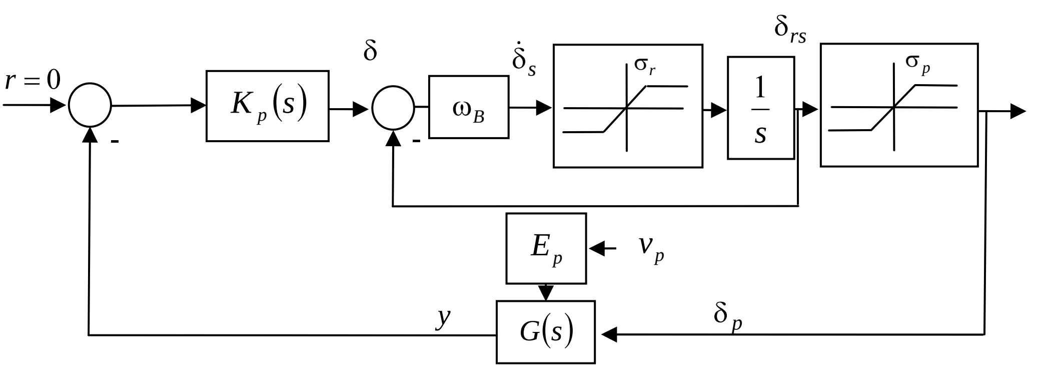

Fig. 2 – Block diagram of the realistic system with position and rate saturations

The next step of the synthesis, represented by the explicit determination of the matrices in (11), (12), supposes an attentive procedure for the selection of the key parameters defined by the noise covariance W_u, V_y and τ, τ_η, Q_y, r in order to obtain the signal noise ratios of $V_u / \sigma^2_{v_u} = \pi \times 0.003$ and $V_{y_i} / \sigma^2_{y_i} = \pi \times 0.01$, which correspond to normalized control noise and normalized observation noise ratios of −25 dB and −20 dB, respectively [5].

It is worthy to note that the covariance value P of the state vector in (11), given by the Lyapunov equation

$$A_{cl} P + P A_{cl}^{\mathrm{T}} + E_{cl} Q E_{cl}^{\mathrm{T}} = 0, \ Q = \mathrm{diag}(W_1, V_y) \quad (13)$$

and the covariance of the vector $Y^{\mathrm{T}} = \begin{bmatrix} y_0 & u_c \end{bmatrix}^{\mathrm{T}}$, given by the Lyapunov equation

$$E\left[YY^{\mathrm{T}}\right]=C_{cl}PC_{cl}^{\mathrm{T}}+Q_{\tilde{v}_y} \tag{13′}$$

will be used in the scheme of fitting the HLQG type pilot model.

3. ADAPTING SEMIGLOBAL STABILIZATION THEORY FOR THE SYSTEM WITH BOTH POSITION AND RATE ACTUATOR SATURATIONS

A typical block diagram for the study of category PIO I-II is shown in Fig. 2. Herein, two basic nonlinearities, usual in flight control, are involved: the position saturation, related to the control stick displacement limits (corresponding to flight control surface rotation limits) and the rate saturation, mainly related to flow rate limits of the hydraulic servo actuator). In figure, specifically to the auto-oscillation searching, $r=0$ is the null reference. $K_p(s)$ is the model of the pilot, δ is the control signal elaborated by the pilot and $y(s)$ is the vector of displayed variables

$$\delta(s)=C_p\left(sI-A_p\right)^{-1}B_py+C_p\left(sI-A_p\right)^{-1}B_pE_pv_p:=K_p(s)y(s)+K_p(s)E_pv_p \tag{14}$$

$\delta_p=\sigma_p(\delta_{rs})$ is the effective control and $G(s)$ is the model of aircraft. σ_p and σ_r are the positions and the rate saturations functions of the actuator, respectively, see Fig. 2. The angular frequency ω_B is in connection with the time constant of the actuator $\tau_e=1/\omega_B$, and σ_p saturation is related to the flight control surface limits. Therefore, in the ideal case – without saturations – a state variable δ_s of the actuator has to be added to the aircraft mathematical model

$$\dot{\delta}_s+\omega_B\delta_s=\omega_B\delta \tag{15}$$

With saturations, the system (5′), thus without including the first order actuator equation (15), will be rewritten as follows:

$$\dot{x}_s=A_sx_s+B_s\sigma_p\left(\delta_{rs}\right)+E_sw_1,\ \dot{\delta}_{rs}=\sigma_r\left(\omega_B\left(\delta-\delta_{rs}\right)\right),\ y_0=C_sx_s+v_y \tag{16}$$

The following family of controllers (see [15]; herein, the considered estimator is the Kalman estimator) solves *the problem of semi global stabilization* [14] as applied to the system (16), with the amendment of ensuring only locally stability, instead of asymptotically stability, taking into account the presence of the noises in system

$$\begin{gathered}\delta=C_d\left(sI-A_d\right)^{-1}\left(B_du_c+E_dv_u\right),\ u_c=-r^{-1}B_s^{\mathrm{T}}K\hat{x}_s/\varepsilon^2-\left(1/\varepsilon^2-1\right)\delta_{rs}\\ 0=A_s^{\mathrm{T}}K+KA_s+Q(\varepsilon)-KB_sr^{-1}B_s^{\mathrm{T}}K,\ Q:=C_s^TQ_y[\varepsilon]C_s\\ \dot{\hat{x}}_s=A_s\hat{x}_s+F\left(y_0-C_s\hat{x}_s\right),F=SC_s^{\mathrm{T}}V_y^{-1},0=A_sS+SA_s^T+W_1-SC_s^{\mathrm{T}}V_y^{-1}\boldsymbol{C}_sS\end{gathered} \tag{17}$$

thus with gains given by Riccati equations. For conformity, usual hypotheses must work: 1) the pair $\left(A_s,B_s\right)$ is stabilizable; 2) all eigenvalues of A_s are located in the closed left half plane; 3) the pair $\left(C_s,A_s\right)$ is detectable. For the case $\varepsilon=1$, the nominal case of the saturation corrections missing, the control (3), (2), (7) is recovered.

The solution (17) starts from the parameterization of the state weight matrix Q_y by a single parameter $\varepsilon \in (0,1]$

$$A_s^{\mathrm{T}} K + K A_s - K B_s r^{-1} B_s^{\mathrm{T}} K = -Q(\varepsilon) \tag{18}$$

where $Q(\varepsilon) = C_s^{\mathrm{T}} Q_y(\varepsilon) C_s$. The properties of the solution $K(\varepsilon)$ are: 1) $\lim_{\varepsilon \to 0} K := K(\varepsilon) = 0$; 2) there exists a constant $\alpha > 0$, such that $\left\| K^{1/2} A_s K^{1/2} \right\| \le \alpha$, with α independent of ε. In this context, the problem of semi global stabilization concerns the finding of a linear control law, parameterized by $\varepsilon \in (0,1]$, so that the closed-loop system satisfies the following criteria: a) the equilibrium point $x = 0$ is locally uniformly exponentially stable for any fixed $\varepsilon \in (0,1]$; b) for any arbitrary large, bounded and a priori given set of state initial conditions X there exists an $\varepsilon^* \in (0,1]$ such that X is contained in the region of attraction for any fixed $\varepsilon \in (0, \varepsilon^*]$.

4. NUMERICAL SIMULATIONS

Let's now consider the case of human pilot performing the hovering control of a VTOL-type aircraft [5]-[8]. Briefly, the pilot's task was to minimize longitudinal position errors while hovering in turbulent air. The approach in the cited references is that of ignoring in estimation/measurement of any information about control. In other words, the matrix D (see below) is taken as a null matrix. Our approach will be different. The lesson derived from the controller (17), as a first step in the development of a more realistic model of the pilot, suggests the insertion of the control variable in the measurement equation (see the feedback component on δ_{rs}). Consequently, the aircraft model and the displayed outputs for the experiment deployment were easily modified by considering the δ_s state and $D \neq 0$

$$\begin{bmatrix} \dot{u}_g \\ \dot{u} \\ \dot{x}_h \\ \dot{q} \\ \dot{\theta} \\ \dot{\delta}_s \end{bmatrix} = \begin{bmatrix} -\omega_{u_g} & 0 & 0 & 0 & 0 & 0 \\ X_u & X_u & 0 & 0 & -g & 0 \\ 0 & 1 & 0 & 0 & 0 & 0 \\ M_u & M_u & 0 & M_q & 0 & M_\delta \\ 0 & 0 & 0 & 1 & 0 & 0 \\ 0 & 0 & 0 & 0 & 0 & -1/\tau_e \end{bmatrix} \begin{bmatrix} u_g \\ u \\ x_h \\ q \\ \theta \\ \delta_s \end{bmatrix} + \begin{bmatrix} 0 \\ 0 \\ 0 \\ 0 \\ 0 \\ 1/\tau_e \end{bmatrix} \delta + \begin{bmatrix} 1 \\ 0 \\ 0 \\ 0 \\ 0 \\ 0 \end{bmatrix} w := Ax + B\delta + Ew \tag{19}$$

$$A = \begin{bmatrix} -0.314 & 0 & 0 & 0 & 0 & 0 \\ -0.1 & -0.1 & 0 & 0 & -9.81 & 0 \\ 0 & 1 & 0 & 0 & 0 & 0 \\ 0.068 & 0.068 & 0 & -3 & 0 & 16.968 \\ 0 & 0 & 0 & 1 & 0 & 0 \\ 0 & 0 & 0 & 0 & 0 & -20 \end{bmatrix} \tag{19'}$$

$$B = \begin{bmatrix} 0 & 0 & 0 & 0 & 0 & 20 \end{bmatrix}^T$$

$$\begin{bmatrix} u \\ x_h \\ q \\ \theta \\ u_c \end{bmatrix} = \begin{bmatrix} 0 & 1 & 0 & 0 & 0 & 0 \\ 0 & 0 & 1 & 0 & 0 & 0 \\ 0 & 0 & 0 & 1 & 0 & 0 \\ 0 & 0 & 0 & 0 & 1 & 0 \\ 0 & 0 & 0 & 0 & 0 & 0 \end{bmatrix} \begin{bmatrix} u_g \\ u \\ x_h \\ q \\ \theta \\ \delta_s \end{bmatrix} + \begin{bmatrix} 0 \\ 0 \\ 0 \\ 0 \\ 1 \end{bmatrix} u_c, \text{i.e., } y = Cx + Du_c \tag{20}$$

The notations concern: u_g − longitudinal component of the gust velocity [m/s]; u − velocity perturbation $\dot{x}_h$ along the x axis [m/s]; θ − pitch attitude [rad]; $q = \dot{\theta}$ − pitch rate, rad/s; δ − control stick input [m]; δ_s − actuator state variable [m]; M_u − speed stability parameter [rad/m/s]; M_q − pitch rate damping [1/sec]; M_δ − control sensitivity [rad/sec^2/m]; X_u − longitudinal drag parameter [1/sec]; g − gravitational constant, 9.81 [m/s^2]; τ_e − actuator time constant (0.05 sec); ω_{u_g} − white noise filter pole [rad/s]. The index (6) will be so recalculated

$$\begin{gathered} J_p = \mathrm{E}_\infty \left\{ y^{\mathrm{T}} Q_y y + u_c^2 r \right\} = \mathrm{E}_\infty \left\{ x^{\mathrm{T}} C^{\mathrm{T}} Q_y C x + 2 u_c D^{\mathrm{T}} Q_y C x + \left(D^{\mathrm{T}} Q_y D + r \right) u_c^2 \right\} \\ Q_y := \mathrm{diag}\begin{pmatrix} 0 & 1 & 400 & 0 & \rho_{u_c} \end{pmatrix}, Q_y := \mathrm{diag}\begin{pmatrix} 0 & 1 & 400 & 0 \end{pmatrix} - \text{nominal case} \end{gathered} \tag{6′}$$

Q_y is in accordance with [5], but with a new tuning parameter ρ_{u_c}. Other synthesis parameters are: $r = 1$; $\tau_\eta = 0.1\,\mathrm{s}$; $\tau = 0.15\,\mathrm{s}$.

Table 1 – Stability margins versus the relation of the constraints in normalized signals ratios

$V_y/\sigma_y^2,\ V_u/\sigma_u^2,\ D \equiv 0$	dB	°
− 20dB, − 25dB (nominal)	5.77	27.6
− 15dB, − 25dB	− 6.7	25.6
− 25dB, − 25dB	6.76	22.4
− 20dB, − 20dB	**6.35**	**31.1**
− 20dB, − 30dB	5.52	25.7

The scenario of numerical experiments supposed: 1) the determination of HLQG pilot model and comparison with the experiments in [5]-[7] in the "nominal" case $D = 0$; 2) the validation of the models by nonlinear simulations (see Fig. 3); 3) the improvement of the pilot mathematical model and its validation with reference to Robust Stability Analysis criterion [21]; a possible approach consists in a voluntary modification of the constraints in normalized signals ratios, see Table 1; 4) another proposed procedure is related to the insertion of the pilot's commanded control between the displayed variables ((20) and (6′)), see Table 2, Fig. 4. A future study concerns the influence of the two approaches on the limit cycles, see Figs. 5, 6.

As concerning the nominal case, the validation of the dynamic pilot model (12) was performed by a simple optimization procedure, having as comparison terms the experimental results given in [5]-[8].

The graphs in Figs. 3, 4 show an acceptable fitness, at least in the interested domain of frequencies, of experimental results versus designed dynamic model. The experimental results are expressed by means of two representative transfer functions Y_θ and Y_x which realize a series loop composed by an inner θ feedback loop and an outer x_h feedback loop. Thus, the machinery of dynamic pilot design is testified.

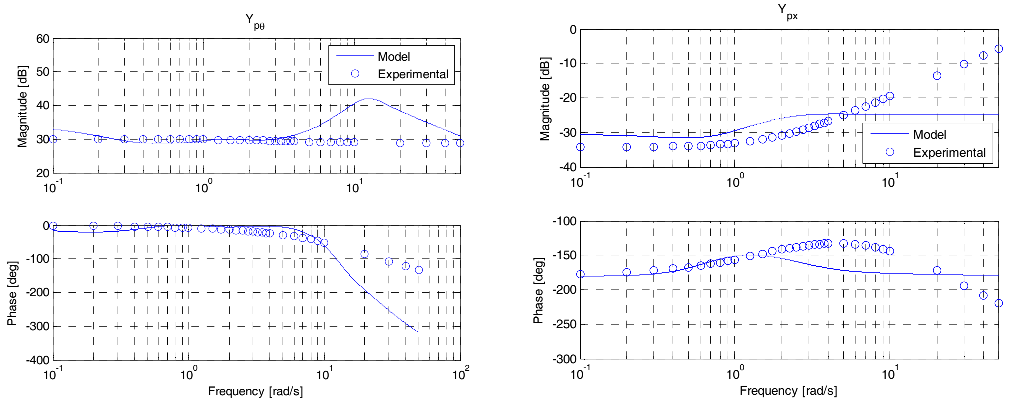

Fig. 3 – Comparison between experimental [5] and HLQG results, case $D = 0$

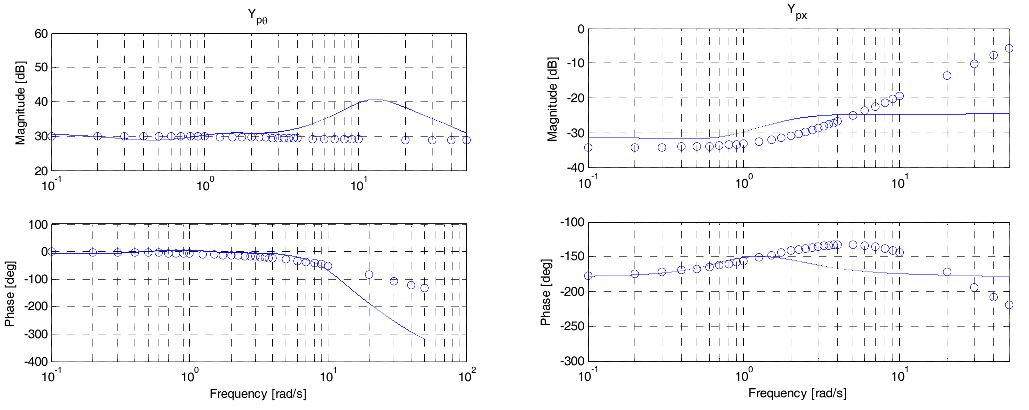

Fig. 4 – Comparison between experimental [5] and HLQG results, case $D \neq 0$

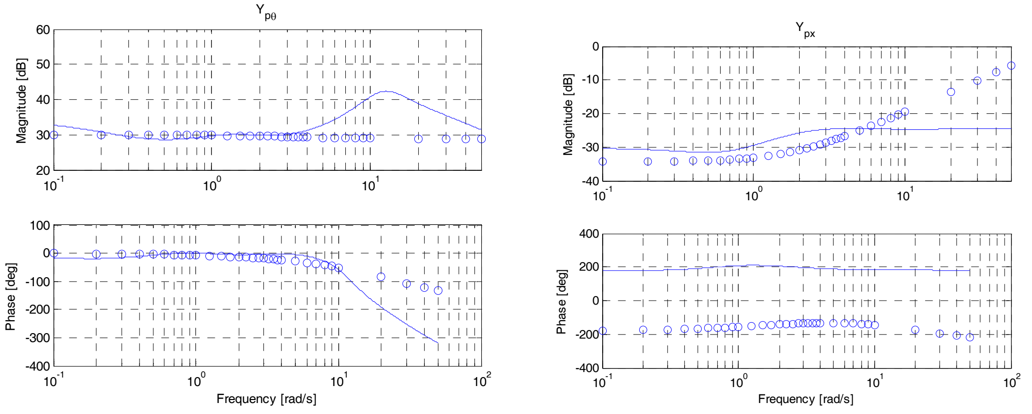

a)

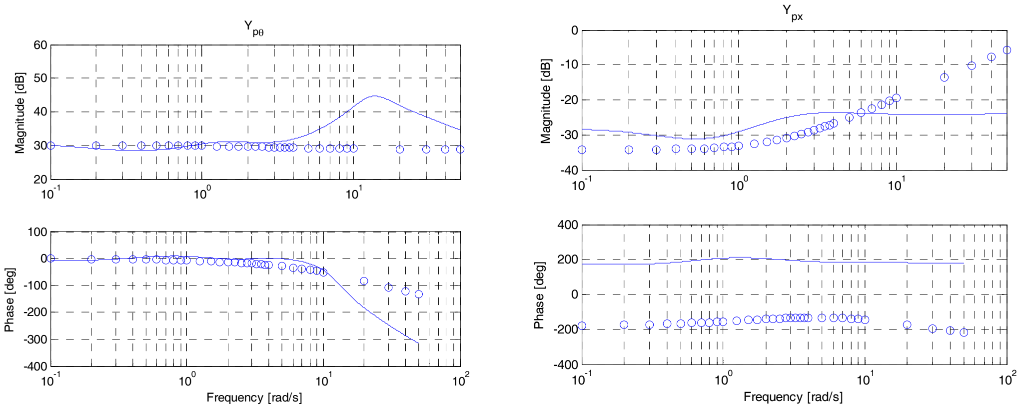

b)

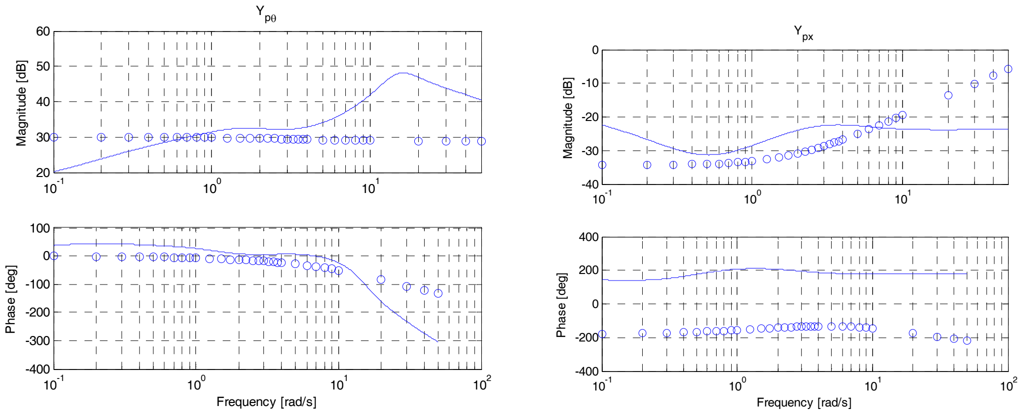

c)

Fig. 4. Comparison between experimental and theoretical results $D \neq 0$ case, $r = 1$

Table 2. Stability margins (dB, ◦) versus the tuning parameter ρ_{u_c}

	dB	◦
$\rho_{uc} = 0.1$ (Fig. 4a)	5.83	28.8
$\rho_{uc} = 1$ (Fig. 4b)	5.77	30.2
$\rho_{uc} = 5$ (Fig. 4c)	5.91	33.9

5. CONCLUDING REMARK

Actuator saturations could lead to instability of the closed loop system pilot-aircraft. The present paper continues recent works of the authors aiming to give a methodology to analyse and predict the emergence of PIO phenomenon.

REFERENCES

[1] F. Amato, R. Iervolino, S. Scala, L. Verde, Actuator design for aircraft robustness versus category PIO, *Proc. of the 7th Mediterranean Conf. on Control and Automation* [*MED 99*], Haifa, Israel, June 28-30, 1999.

[2] D. M. Klyde, D. G. Mitchell, A PIO Case study – Lessons learned through analysis, *AIAA Atmosphere Flight Mechanics Conference and Exhibit*, August 15-18, 2005, San Francisco, California, AIAA 2005-5813.

[3] Toader, A., I. Ursu (2010), PIO I-II tendencies case study. Part 1. Mathematical modeling, *INCAS Bulletin*, vol. **2,** 1, 91-102.

[4] J. B. Davison, D. K. Schmidt, Modified optimal control pilot model for computer-aided design and analysis, *NASA-TM-4384*, 1992.

[5] D. L. Kleinman, S. Baron, Manned vehicle systems analysis by means of modern control theory, *NASA CR-1753*, Washington, D.C., June 1971 (DECLASSIFIED).

[6] E. W. Vinje, D. P. Miller, Interpretation of pilot opinion by application of multiloop models to a VTOL flight simulator task, *NASA SP-144*, March, 1967.

[7] E. W. Vinje, D. P. Mille, An analysis of pilot adaptation in a simulated multiloop VTOL hovering task, *NASA SP-192*, March, 1968.

[8] D. P. Miller, E. W. Vinje, Fixed base flight simulator studies of VTOL aircraft handling qualities in hovering and low-speed flight, *United Aircraft Research Laboratories Report F910482-12*, 1968..

[9] *** Flight Control Design – Best practices, *NATO Technical Report* 29, 2000.

[10] A. Toader, I. Ursu, From limits of human pilot mathematical modeling to actuator rate limits. A PIO II tendencies case study, *Mathematical Methods in Engineering International Symposium, Instituto Politecnico de Coimbra, Portugal*, 21-24 October, 2010, CD published.

[11] H. K. Khalil, *Nonlinear systems*, 3rd edition, Prentice Hall, 2002.

[12] D. Materassi, M. Salapaka, M. Basso, A less conservative circle criterion, *Nonlinear Sciences – Chaos Dynamics*, June 2008; see also in *Proceedings of the 2006 ACC*, Minneapolis, Minnesota, USA, June 14-16, 2006.

[13] E. D. Sontag, H. J. Sussmann, Nonlinear output feedback design for linear systems with saturating actuators, *Proc. 29th CDC*, pp. 3414-3416, 1990.

[14] Z. Lin, A. Saberi, Semi-global exponential stabilization of linear systems subject to input saturation via linear feedback, *Systems & Control Letters*, vol. **21**, no. 3, pp. 225-239, 1993.

[15] Z. Lin, Semi-global stabilization of linear systems with position and rate-limited actuators, *Systems & Control Letters*, vol. **30**, pp. 1-11, 1997.

[16] T. Lauvdal, Stabilization of linear systems with input magnitude and rate saturations, *Thesis*, Depart. of Eng. Cybernetics, Norwegian Univ. of Science and Technology, Trondheim, Norway, 1998.

[17] I. Ursu, F. Ursu, F. Popescu, Backstepping design for controlling electrohydraulic servos, *Journal of The Franklin Institute*, USA, vol. **343**, January, pp. 94-110, 2006.

[18] W. E. Schmittendorf, B. R. Barmish, Null controllability of linear systems with constrained controls, *SIAM J. Control Optimiz.*, vol. **18**, pp. 327-345, 1989.

[19] A. R. Fuller, In-the-large stability of relay and saturating control systems with linear controller, *Int. J. Control*, vol. **10**, pp. 457-480, 1969.

[20] R. A. Hess, Theory for aircraft handling qualities based upon a structural pilot model, *Journal of Guidance, Control, and Dynamics*, **12**, 6, 792-797, 1989.

[21] *** Flight Control Design – Best Practices, *NATO Research and Technology Organization,* TR 029, 2000.